

The optical counterpart to the X-ray transient IGR J1824-24525 in the globular cluster M28¹

C. Pallanca², E. Dalessandro², F.R. Ferraro², B. Lanzoni² and G. Beccari³.

² *Dipartimento di Fisica e Astronomia, Università degli Studi di Bologna, Viale Berti Pichat 6/2, I-40127 Bologna, Italy; cristina.pallanca3@unibo.it*

³ *European Southern Observatory, Karl-Schwarzschild-Strasse 2, 85748 Garching bei München, Germany*

24 Jun, 2013

ABSTRACT

We report on the identification of the optical counterpart to the recently detected INTEGRAL transient IGR J1824-24525 in the Galactic globular cluster M28. From the analysis of a multi epoch HST dataset we have identified a strongly variable star positionally coincident with the radio and Chandra X-ray sources associated to the INTEGRAL transient. The star has been detected during both a quiescent and an outburst state. In the former case it appears as a faint, unperturbed main sequence star, while in the latter state it is about two magnitudes brighter and slightly bluer than main sequence stars. We also detected H α excess during the outburst state, suggestive of active accretion processes by the neutron star.

Subject headings: Binaries: close, Stars: neutron, Globular Cluster: individual (M28), X-ray: individual (IGR J18245-2452)

1. INTRODUCTION

The high stellar densities and the frequent dynamical interactions occurring in globular cluster (GC) cores are expected to significantly affect the formation and the evolution of exotic populations, such as low-mass X-ray binaries (LMXBs), cataclysmic variables, millisecond pulsars (MSPs), and blue straggler stars (e.g. Bailyn 1995; Verbunt et al.

¹Based on observations collected with the NASA/ESA HST (Prop. 19835), obtained at the Space Telescope Science Institute, which is operated by AURA, Inc., under NASA contract NAS5-26555.

1997; Grindlay et al. 2001; Pooley et al. 2003; Ferraro et al. 2009). In fact, these objects are thought to result from the evolution of various kinds of binary systems originated and/or hardened by stellar interactions (e.g. Clark 1975; Hills & Day 1976; Bailyn 1992; Ivanova et al. 2008), and are therefore considered as powerful diagnostics of GC dynamical evolution (e.g. Ferraro et al. 1995; Goodman & Hut 1989; Hut et al. 1992; Meylan & Heggie 1997; Pooley et al. 2003; Fregeau 2008; Ferraro et al. 2012). However, many open questions still remain about their formation and evolutionary paths.

When a close binary system contains a compact object, mass transfer processes can take place. The streaming gas, its impact on the compact star, or the presence of an accretion disk can produce significant X-ray and UV radiation, together with emission lines (such as the $H\alpha$) or rapid luminosity variations. The first evidence of interacting binaries in Galactic GCs was indeed obtained through the discovery of X-ray sources. In particular, LMXBs are thought to be binary systems with an accreting neutron star (NS) and are characterized by X-ray luminosities larger than $\sim 10^{35}$ erg s $^{-1}$. Their final stage is thought to be a binary system containing a very fast NS (a MSP), spun up through mass accretion from the evolving companion. Moreover, during their life some LMXBs, usually called X-ray transients (White et al. 1984), show a few outbursts and during the quiescent state their millisecond pulsation can become detectable (Chakrabarty & Morgan 1998).

The identification of the optical counterparts is a fundamental step for characterizing these exotic binary systems, both in quiescent and in outburst state, and for clarifying their formation and evolutionary processes (Testa et al. 2012). Determining the nature and the properties of the companion (which dominates the optical emission in the quiescent state) is also very useful to tightly constrain the orbital parameters of the system (e.g. D’Avanzo et al. 2009; Engel et al. 2012). In the case of GCs, it also represents a crucial tool for quantifying the occurrence of dynamical interactions, understanding the effects of crowded stellar environments on the evolution of binaries, and determining the shape of the GC potential well (e.g. Phinney 1992; Bellazzini et al. 1995; Possenti et al. 2003; Ferraro et al. 2003).

M28 (NGC 6626) is a Galactic GC with intermediate central density ($\log \rho_0 = 4.9$ in units of $M_\odot \text{pc}^{-3}$; Pryor & Meylan 1993) and relatively high metallicity ($[\text{Fe}/\text{H}] = -1.32$, Harris 1996, 2010 version) located at ~ 6.8 kpc from Earth, in the direction of the Galactic centre (Harris 1996). It is the first Galactic GC where a MSP was discovered (Lyne et al. 1987) and it is currently known to host the third largest population of pulsars among all GCs (Bégin 2006; Bogdanov et al. 2011)². A total of 46 X-ray sources, of which 12 lie within

²For the complete list of pulsars in Galactic GCs unambiguously see the web site <http://www.naic.edu/~pfreire/GCpsr.html>

one core radius ($r_c = 14.4''$; Harris 1996) from the centre, has been detected with Chandra (Becker et al. 2003).

During the observations of the Galactic center performed on 2013 March 28 with INTEGRAL, a new hard X-ray transient (IGR J18245-2452) has been revealed in the direction of M28 (Eckert et al., ATel #4925). Subsequent observations with SWIFT/XRT confirmed the detection of the transient source and its location within the core of the cluster, at $\alpha_{2000} = 18^{\text{h}}24^{\text{m}}32.20^{\text{s}}$ and $\delta_{2000} = -24^{\circ}52'05.5''$, with error radius $3.5''$ (at 90% confidence; Heinke et al., ATel #4927; Romano et al., ATel #4929). SWIFT/XRT time-resolved spectroscopy performed on 2013 April 7 have revealed a thermal spectrum with a “cooling tail”, unambiguously identifying the burst as thermonuclear and suggesting that the source is a low-luminosity LMXB in the hard state, where a NS is accreting matter from a companion (Linares, Atel. #4960; see also Serino et al., Atel #4961). A radio follow-up has been performed with ATCA on 2013 April 5, for a total of 6 hours, at two different frequencies (9 and 5.5 Hz). A single source has been identified at $\alpha_{2000} = 18^{\text{h}}24^{\text{m}}32.51^{\text{s}}$ and $\delta_{2000} = -24^{\circ}52'07.9''$, with a 90% confidence error of $0.5''$ (Pavan et al., ATel #4981). This position is only marginally consistent with that derived from the SWIFT/XRT data, but the detected strong variability (reaching up to 2.5 times the mean flux density during the first 90 minutes of observations) suggests a possible association with the X-ray transient. Its position well corresponds to the location of the X-ray source #23 identified by Becker et al. (2003) from Chandra observations and associated to IGR J1824-24525 by Homan et al. (ATel #5045).

Here we report on the identification of the optical counterpart to IGR J1824-24525, obtained from the analysis of high resolution HST data acquired with the WFPC2, WFC3 and ACS/WFC in three different epochs (see also Pallanca et al. Atel#5003, and Cohn et al. Atel #5031). In Section 2 we describe the dataset and the data analysis procedure. The properties of the optical counterpart to IGR J1824-24525 are presented in Section 3 and discussed in Section 4.

2. OBSERVATIONS AND DATA ANALYSIS

For this work we adopted the same catalog used to identify the companion to PSR J1824-2452H and fully described in Pallanca et al. (2010). In order to unveil luminosity variations among different epochs, two additional sets of HST data acquired with the WFPC2 and the ACS have been analyzed. In particular, because we were interested only in the GC core, we limited the analysis to the Planetary Camera (PC) of the WFPC2 and CHIP2 of the ACS/WFC mosaic. The available samples have been acquired through various filters, at

three different epochs (see Table 1): the WFPC2 dataset was collected on 2009, April 7 (epoch 1, hereafter EP1), WFC3 observations were performed on 2009, August 9 (epoch 2, EP2) and the ACS data-set was acquired on 2010, April 26 (epoch 3, EP3).

The data reduction procedure for the ACS sample has been performed on the CTE-corrected (flc) images, once corrected for Pixel-Area-Map (PAM) by using standard IRAF procedures. The photometric analysis has been carried out by using the DAOPHOT package (Stetson 1987). For each image we modeled the point spread function (PSF) by using a large number (~ 100) of bright and nearly isolated stars. Then, all F435W and F625W images have been combined with MONTAGE2 and used to produce a master frame on which we optimized a master list of stars. Finally we performed the PSF fitting on this master list by using the DAOPHOT packages ALLSTAR and ALLFRAME (Stetson 1987, 1994). A similar procedure has been adopted to reduce the flat-fielded (flt) WFPC2 images.

Since the ACS images heavily suffer from geometric distortions within the field of view, we corrected the instrumental positions of stars by applying the equations reported by Sirianni et al. (2005). We then placed, through cross-correlation, the ACS and the WFPC2 data sets on the same astrometric system of the WFC3 sample, for which the astrometric solution has an accuracy of $\sim 0.2''$ in both right ascension and declination (Pallanca et al. 2010).

Finally, the instrumental magnitudes have been calibrated to the VEGAMAG system by using the photometric zero-points reported on the instrument web pages³ and the procedure described in Holtzman et al. (1995) and Sirianni et al. (2005) for WFPC2 and ACS, respectively.

3. THE OPTICAL COUNTERPART TO IGR J18245-2452

During a systematic study of the GC M28 aimed at searching for the companion stars to binary MSPs, we found a peculiar object (see Figure 1) located at $\alpha_{2000} = 18^{\text{h}}24^{\text{m}}32.50^{\text{s}}$ and $\delta_{2000} = -24^{\circ}52'07.8''$, in very good agreement with the position of the X-ray source #23 reported by Becker et al. (2003) and of the variable ATCA radio source discussed by Pavan et al. (Atel #4981).

In EP2 this star showed a strong and irregular variability in each filter, on a timescale

³www.stsci.edu/hst/acs/analysis/zeropoints/zpt.py and www.stsci.edu/documents/dhb/web/c32-wfpc2/dataanal.fm1.html for ACS and WFPC2, respectively

of ~ 10 hours (Figure 2). Based on the mean magnitudes⁴ (F390W= 20.61 ± 0.01 , F606W= 19.45 ± 0.02 , F814W= 18.83 ± 0.03 and F656N= 17.42 ± 0.02), this star turns out to be about 0.5-1 magnitude fainter than the main sequence (MS) turn off (TO) and bluer than the MS both in the (F390W, F390W-F606W) and in the (F606W, F606W-F814W) color magnitude diagrams (CMDs; see Figure 3). Even more interesting is the comparison of the photometric properties among the three epochs of observations. Unlike the CMD location in EP2, the magnitudes derived for EP1 (F555W= 21.17 ± 0.06 and F336W= 23.04 ± 0.21) and for EP3 (F435W= 22.50 ± 0.03 , F625W= 20.60 ± 0.03 and F658N= 20.27 ± 0.03) approximately locate the star onto the MS. Unfortunately, given the different instruments and filters, it is not possible to directly compare the magnitudes but, both from the visual inspection of images (see Figure 1) and from the CMD locations with respect to the TO point, it turns out that during EP1 and EP3 the star was about 2-3 magnitudes fainter than the TO, and hence ~ 2 mag fainter than in EP2. This likely indicates that the observations during EP1 and EP3 sampled the object in quiescence, while EP2 data caught the star in an outburst state. In addition, during each epoch a magnitude modulation is present, with an indication of a smaller amplitude in EP3 with respect to the variability detected during the EP2 outbursting state. In fact, the frame-to-frame magnitude scatter of the peculiar star during the outburst epoch (EP2) is $10 - 20\sigma$ larger than the scatter of normal stars in the same magnitude bin, while this value decreases to $\sim 4\sigma$ in EP3.

In principle, for actively accreting LMXBs, $H\alpha$ emission is expected from the accretion disk, while the contribution from the heated companion star should be minimal or even absent. A visual inspection of EP2 images already suggests that this peculiar star also has $H\alpha$ excess: in fact, in the F656N image (panel (e) in Figure 1) it is significantly brighter than its southern neighbor, while these two objects show essentially the same magnitude in broad band filters (as the F390W, see panel (b) in Figure 1). In order to quantify this excess we used a photometric technique based on the comparison between the magnitudes obtained from broad band and $H\alpha$ narrow filters (Cool et al. 1995). In particular, in this work we used a method commonly applied to star forming regions (De Marchi et al., 2010) and recently tested for the first time in the GC 47Tucanae (Beccari et al., MNRAS submitted; see also Beccari et al. 2013). First of all, we corrected all magnitudes for reddening by adopting $E(B - V) = 0.4$ (Harris 1996), then we selected the peculiar star in the (F606W-F656N)₀ vs (F606W-F814W)₀ color-color diagram. Note that this color combination well samples the continuum of stars with no $H\alpha$ emission for different spectral types through the (F606W-

⁴It is important to note that, given the variability and an undersampled time coverage, the mean magnitudes (and hence the colors) derived here could not exactly correspond to the true average luminosities of the star over the entire variability period.

$F814W)_0$ color index, and it provides a good estimate of the $H\alpha$ emission through the $(F606W-F656N)_0$ color index, since the $H\alpha$ line contribution to the $F606W$ band is negligible. The $H\alpha$ excess ($\Delta H\alpha$) can be evaluated from the distance between the $(F606W-F656N)_0$ color index of the considered star and an empirical line⁵ representative of the continuum. In addition, the equivalent width (EW) of the $H\alpha$ emission can be quantitatively estimated from $\Delta H\alpha$ by applying equation (4) in De Marchi et al. (2010): $EW_{H\alpha} = RW \times [1 - 10^{-0.4 \times \Delta H\alpha}]$, where RW is the rectangular width of the filter, (see Table 4 in De Marchi et al. 2010). With such a method we estimated the $H\alpha$ excess ($\Delta H\alpha = 1.98 \pm 0.03$; upper panel in Figure 4) and the EW of the $H\alpha$ emission ($EW_{H\alpha} = 71.6_{-5.1}^{+5.5}$ Å, where the uncertainties take into account the errors in both colors) during the EP2 outburst state. By applying an analogous method to EP3 data, making use of a suitable combination of $F435W$, $F625W$ and $F658N$ filters, we find that the star is located on the continuum reference line during its quiescent state (see the lower panel in Figure 4). Hence there is no indication of $H\alpha$ emission in that epoch.

Finally, we tried to investigate the possible presence of UV emission by using the EP1 dataset in filters $F255W$ and $F170W$. No source is detected at the location of the peculiar star, most probably because the images are not deep enough to reach its faint magnitudes.

4. DISCUSSION AND CONCLUSIONS

The photometric analysis revealed the presence of a very peculiar star, which underwent a strong luminosity increase and showed significant $H\alpha$ excess in EP2. Even if this optical outburst occurred a few years before the INTEGRAL discovery, this evidence, combined with the positional coincidence with the ATCA variable source recently detected by Pavan et al. (Atel #4981) and with the Chandra X-ray source #23 revealed by Becker et al. (2003) and firmly associated to IGR J1824-24525 by Homan (Atel #5045), strongly suggests that we have identified the optical counterpart to IGR J1824-24525. Indeed several outbursts separated by a few years delay are quite typical of LMXBs containing a NS (e.g 4U 1608-52, Aquila X-1; Asai et al. 2012).

Unlikely, the poor and irregular time coverage of our data prevented us to firmly de-

⁵The reference line for the continuum has been determined from the median $(F606W-F656N)_0$ color as function of $(F606W-F814W)_0$ for stars with combined photometric error smaller than 0.05 magnitudes. As shown in Figure 4, this empirical relation agrees very well with the theoretical one, obtained from atmospheric models (Bessell et al. 1998). We also emphasize that, while M28 may be affected by mild differential reddening, the reddening vector is almost parallel to the empirical line tracing the continuum (see Figure 4). This means that even large fluctuations in the reddening of individual stars would not significantly affect the identification of objects with $H\alpha$ excess (Beccari et al. 2010).

termine the period of the magnitude modulation, which is expected to be correlated with the binary orbital motion. However, the non regular shape of the light curve (likely due to an insufficient sampling of the orbital period), seems to suggest that the variability is occurring in a timescale a few times shorter than the duration of the observations ($\sim 5 - 10$ hours). This seems to be in agreement with the known properties of previously identified low mass X-ray transients, that have orbital periods in the range between 40 min and 4.3 hours (D’Avanzo et al. 2009) and even shorter in GCs (Homer et al. 2001; Zurek et al. 2009, and reference therein).

During the quiescent state the companion star is approximately located on the MS, ~ 3 magnitudes fainter than the TO, while during the outburst it is ~ 2 magnitudes brighter and it is characterized by a bluer color. As known from the study of companions to MSPs and LMXBs, such an anomalous position is indicative of a perturbed state (see, e.g. Ferraro et al. 2001; Cocozza et al. 2008; Pallanca et al. 2010; Testa et al. 2012). In fact tidal deformations, heating processes and the presence of an accretion disk can significantly affect the magnitude and temperature of the star (E. Dalessandro et al., in preparation), thus also altering its position in the CMDs. The main tool to discriminate between these effects is the determination of the light curve shape, but the available data-sets prevent us to perform this study.

Finally, the presence of strong $H\alpha$ emission (with $EW_{H\alpha} = 71.6_{-5.1}^{+5.5}$ Å) during the outburst phase suggests the presence of material accreting onto the NS. On the other hand, no $H\alpha$ has been detected in quiescence, in agreement with the fact that when the accretion rate is slow, the disk is much weaker and the $H\alpha$ absorption from the companion star dominates the spectrum.

Further optical studies are required to better constrain this system. First of all, a photometric follow up, with a suitable time sampling is needed to obtain accurate light curves and hence constrain the orbital parameters of the system. Also a spectroscopic analysis, that, given the high crowding and the relative faint magnitude, is possible only during a bright state, could help to characterize such system and the possible presence of an accretion disk through the study of the radial velocity curve, the chemical abundance patterns and UV emission lines. However to properly derive the companion radial velocity curve, it is needed to detect the spectral lines associated with the companion and to avoid those coming from the accretion disk.

After the submission of this paper, XMM observations suggested that IGR J18245-2452 is the same source observed in the radio band as PSR J1824-2452I (Papitto et al., arXiv:1305.3884v1).

5. Acknowledgement

This research is part of the project COSMIC-LAB (www.cosmic-lab.eu) funded by the European Research Council (under contract ERC-2010-AdG-267675). GB acknowledges the European Community's Seventh Framework Programme under grant agreement no. 229517.

REFERENCES

- Asai, K., Matsuoka, M., Mihara, T., et al. 2012, PASJ, 64, 128
- Bailyn, C. D. 1992, ApJ, 392, 519
- Bailyn, C. D. 1995, ARA&A, 33, 133
- Beccari, G., Spezzi, L., De Marchi, G., et al. 2010, ApJ, 720, 1108
- Beccari, G., De Marchi, G., Panagia, N., & Pasquini, L. 2013, IAU Symposium, 290, 187
- Becker, W., Swartz, D. A., Pavlov, G. G., et al. 2003, ApJ, 594, 798
- Bégin, S., M.Sc. thesis, Dept. of Physics and Astronomy, University of British Columbia (2006).
- Bellazzini, M., Pasquali, A., Federici, L., Ferraro, F. R., & Pecci, F. F. 1995, ApJ, 439, 687
- Bessell, M. S., Castelli, F., & Plez, B. 1998, A&A, 333, 231
- Bogdanov, S., van den Berg, M., Servillat, M. et al. 2011, ApJ, 730, 81
- Chakrabarty, D., & Morgan, E. H. 1998, Nature, 394, 346
- Clark, G. W. 1975, ApJ, 199, L143
- Cocozza, G., Ferraro, F. R., Possenti, A., et al. 2008, ApJ, 679, L105
- Cool, A. M., Grindlay, J. E., Cohn, H. N., Lugger, P. M., & Slavin, S. D. 1995, ApJ, 439, 695
- D'Avanzo, P., Campana, S., Casares, J., et al. 2009, A&A, 508, 297
- De Marchi, G., Panagia, N., & Romaniello, M. 2010, ApJ, 715, 1
- Engel, M. C., Heinke, C. O., Sivakoff, G. R., Elshamouty, K. G., & Edmonds, P. D. 2012, ApJ, 747, 119

- Ferraro, F. R., Fusi Pecci, F., & Bellazzini, M. 1995, *A&A*, 294, 80
- Ferraro, F. R., Possenti, A., D’Amico, N., & Sabbi, E. 2001, *ApJ*, 561, L93
- Ferraro, F. R., Possenti, A., Sabbi, E., Lagani, P., Rood, R. T., D’Amico, N., & Origlia, L. 2003, *ApJ*, 595, 179
- Ferraro, F. R., Beccari, G., Dalessandro, E., et al. 2009, *Nature*, 462, 1028
- Ferraro, F.R. et al., 2012, *Nature*, 492, 393
- Fregeau, J. M. 2008, *ApJ*, 673, L25
- Goodman, J., & Hut, P. 1989, *Nature*, 339, 40
- Grindlay, J. E., Heinke, C., Edmonds, P. D., & Murray, S. S. 2001, *Science*, 292, 2290
- Harris, W. E. 1996, *AJ*, 112, 1487
- Hills, J. G., & Day, C. A. 1976, *Astrophys. Lett.*, 17, 87
- Holtzman, J. A., Burrows, C. J., Casertano, S., et al. 1995, *PASP*, 107, 1065
- Homer, L., Anderson, S. F., Margon, B., Deutsch, E. W., & Downes, R. A. 2001, *ApJ*, 550, L155
- Hut, P., et al. 1992, *PASP*, 104, 981
- Ivanova, N., Heinke, C. O., Rasio, F. A., Belczynski, K., & Fregeau, J. M. 2008, *MNRAS*, 386, 553
- Lyne, A. G., Brinklow, A., Middleditch, J., Kulkarni, S. R., & Backer, D. C. 1987, *Nature*, 328, 399
- Meylan, G., & Heggie, D. C. 1997, *A&A Rev.*, 8, 1
- Pallanca, C., Dalessandro, E., Ferraro, F. R., et al. 2010, *ApJ*, 725, 1165
- Papitto, A., Ferrigno, C., Bozzo, E., et al. 2013, *arXiv:1305.3884*
- Phinney, E. S. 1992, *Royal Society of London Philosophical Transactions Series A*, 341, 39
- Pooley, D., et al. 2003, *ApJ*, 591, L131
- Possenti, A., D’Amico, N., Manchester, R. N., Camilo, F., Lyne, A. G., Sarkissian, J., & Corongiu, A. 2003, *ApJ*, 599, 475

- Pryor, C., & Meylan, G. 1993, *Structure and Dynamics of Globular Clusters*, 50, 357
- Sirianni, M., Jee, M. J., Benítez, N., et al. 2005, *PASP*, 117, 1049
- Stetson, P. B. 1987, *PASP*, 99, 191
- Stetson, P. B. 1994, *PASP*, 106, 250
- Testa, V., di Salvo, T., D’Antona, F., et al. 2012, *A&A*, 547, A28
- Verbunt, F., Bunk, W. H., Ritter, H., & Pfeffermann, E. 1997, *A&A*, 327, 602
- White, N. E., Kaluzienski, J. L., & Swank, J. H. 1984, *American Institute of Physics Conference Series*, 115, 31
- Zurek, D. R., Knigge, C., Maccarone, T. J., Dieball, A., & Long, K. S. 2009, *ApJ*, 699, 1113

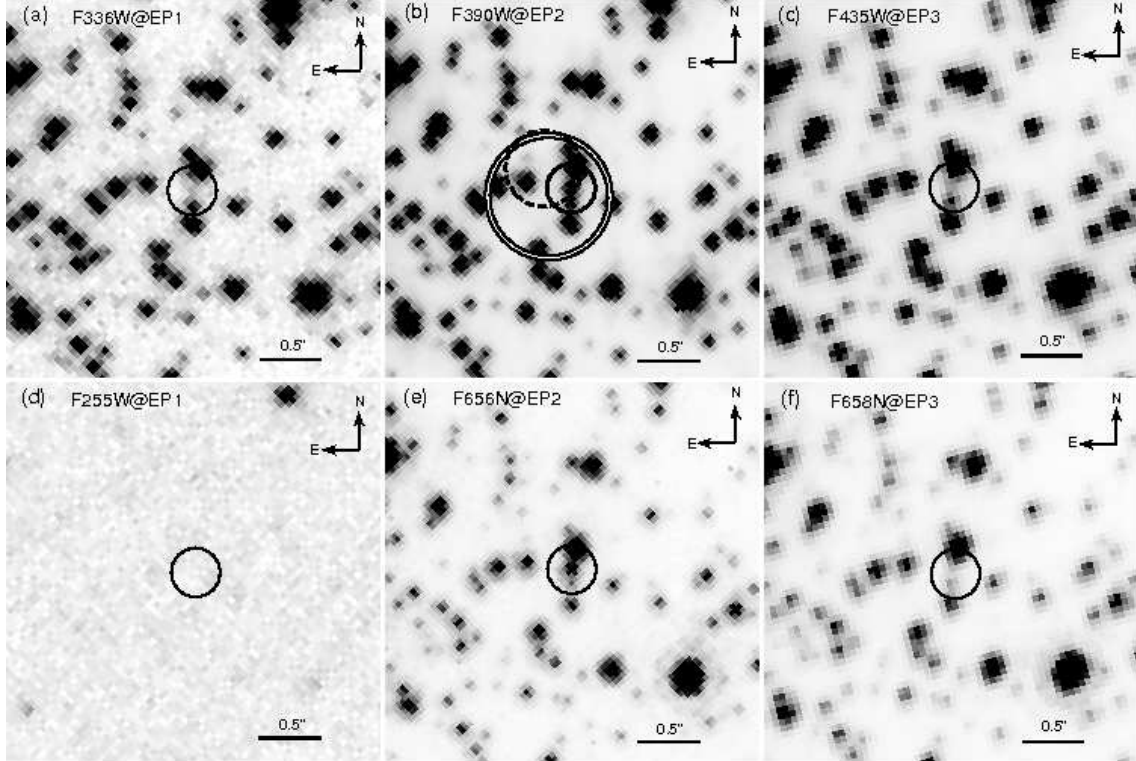


Fig. 1.— HST images of the optical counterpart (solid circle) to IGR J1824-24525. The filters and epochs of observation are labelled in each panel (see Table 1 for more details). Clearly, the source is in a quiescent state in EP1 and EP3 (leftmost and rightmost panels), while it has been caught in outburst during EP2 (central panels). In panel (b) the double and dashed circles mark, respectively, the position of the variable ATCA source detected by Pavan et al. (ATel #4981) and the Chandra X-ray source # 23 (Becker et al. 2003), with the radii corresponding to the quoted astrometric uncertainties.

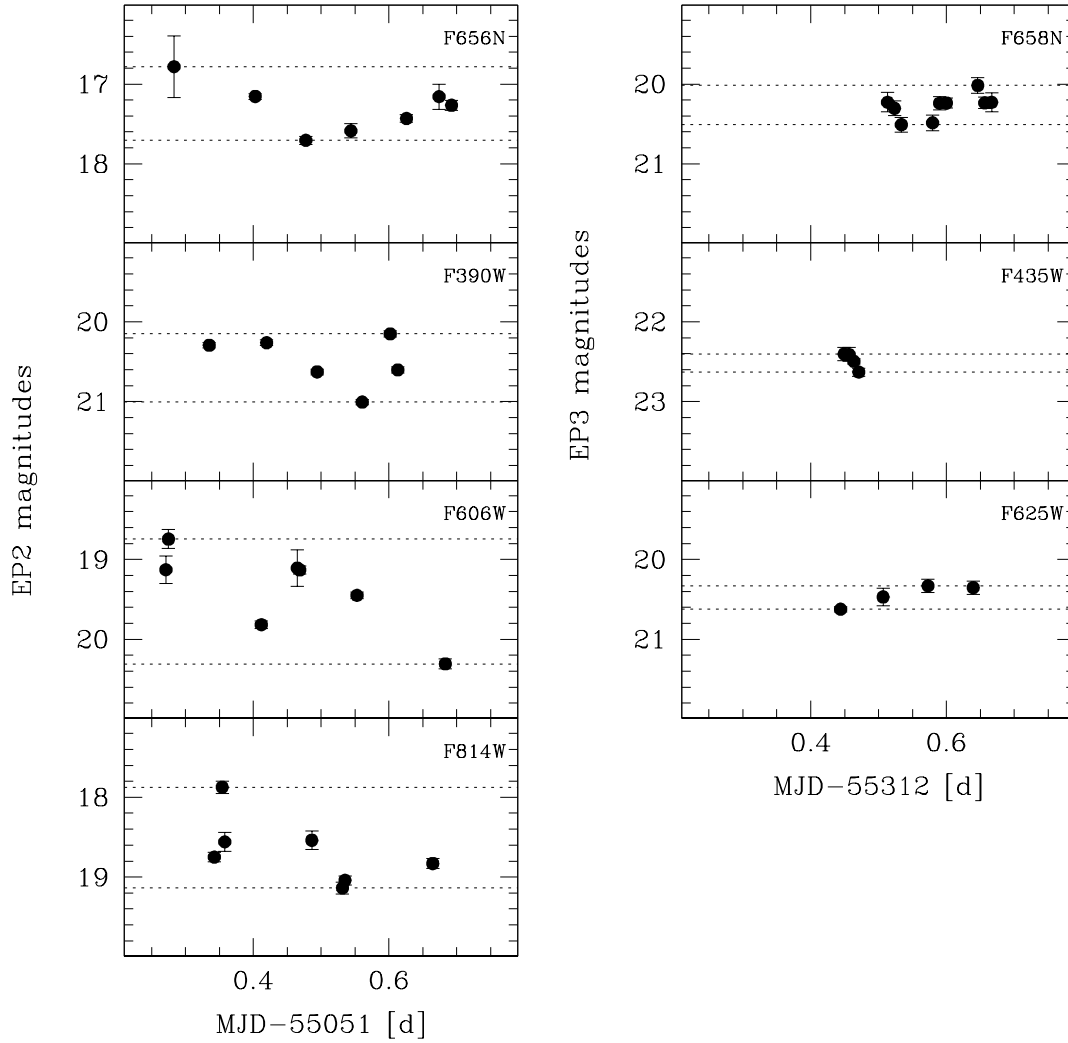


Fig. 2.— Light curves of the optical counterpart to IGR J1824-24525 during the outburst state (left panels) and the quiescent state (right panels). The dotted lines mark the maximum range of variability detected by each set of observations. Photometric errors are reported, but in most cases are smaller than the point size.

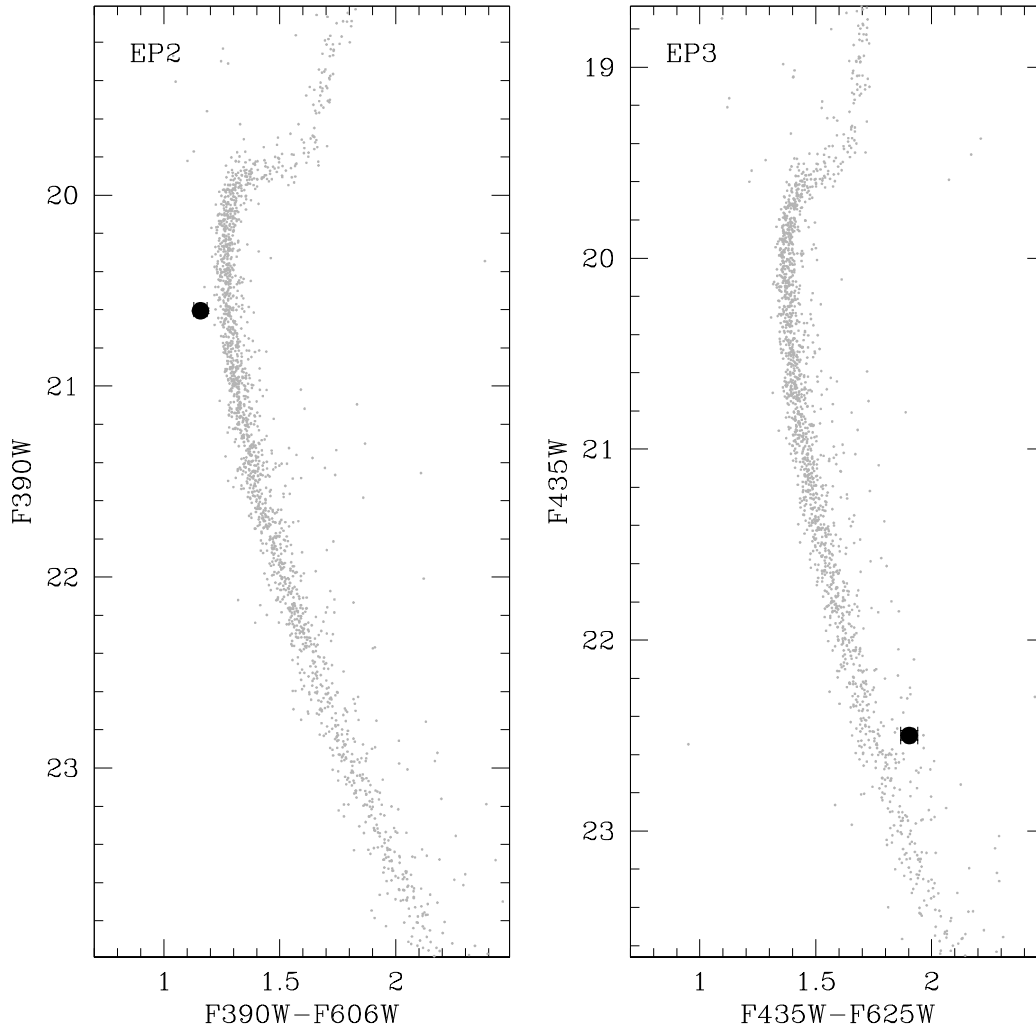


Fig. 3.— Color magnitude diagrams obtained during outburst epoch (left panel) and quiescence epoch (right panel) for all stars (gray points) located within $10''$ from IGR J1824-24525. The location of the optical counterpart to IGR J1824-24525, as obtained by averaging the observed light curves (see Figure 2 and footnote 3), is shown as a large solid circle.

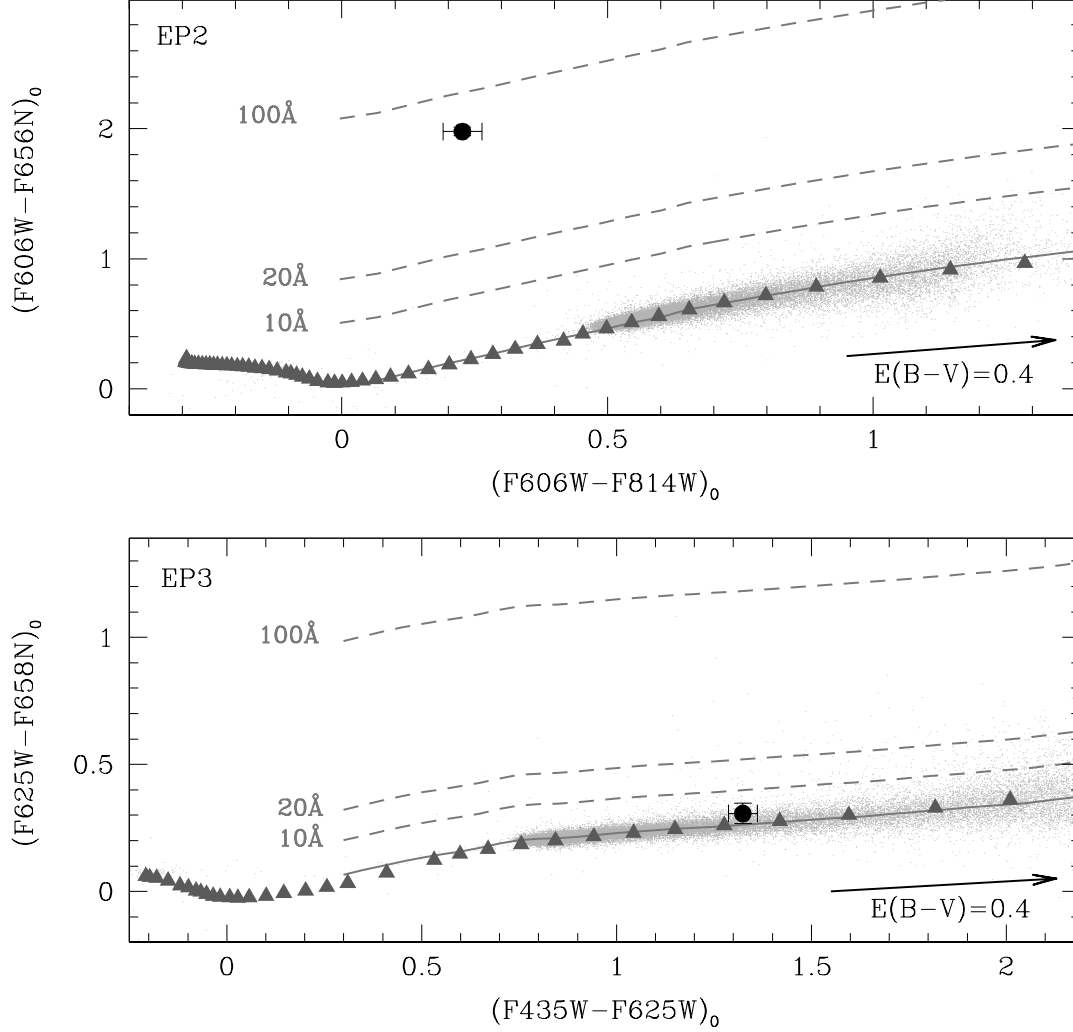


Fig. 4.— Reddening corrected color-color diagrams for both EP2 and EP3. In each panel the solid line is the median color of stars (gray dots) with no $H\alpha$ excess and hence the location of stars with $EW_{H\alpha} = 0$. It well corresponds to the location (gray triangles) predicted from atmospheric models (Bessell et al. 1998). Dashed lines show the expected position for stars with increasing levels of $H\alpha$ emission, with the corresponding $EW_{H\alpha}$ labelled. The black dots mark the positions of the optical counterpart to IGR J1824-24525 in each epoch. During the outburst (upper panel) its $H\alpha$ emission corresponds to $EW_{H\alpha} = 71.6^{+5.5}_{-5.1}$ Å, while in the quiescent state (lower panel) the star is located on the continuum reference line of stars with no $H\alpha$ excess.

Epoch	Date	Instrument	Filter	t_{exp} [s]	State	Proposal ID/PI
EP1	2009/04/07	WFPC2/PC	F170W	2×1700	Q	GO11975/Ferraro
			F255W	3×1200		
			F336W	3×800		
			F555W	2×80		
EP2	2009/08/09	WFC3/UVIS	F390W	$5 \times 850 + 1 \times 800$	B	GO11615/Ferraro
			F606W	7×200		
			F814W	7×200		
			F656N	$2 \times 1100 + 1 \times 1070$		
				$3 \times 1020 + 1 \times 935$		
EP3	2010/04/26	ACS/WFC	F435W	4×464	Q	GO11340/Grindlay
			F625W	4×60		
			F658N	$6 \times 724 + 3 \times 717$		

Table 1: Summary of the multi-epoch data-sets used in this work. The quiescent and outburst state (see Section 3) are marked by letters Q and B, respectively.